MECHANICS OF CRUSTAL EARTHQUAKES

by

W.F. Brace, Principal Investigator

Department of Earth & Planetary Sciences
Massachusetts Institute of Technology
Cambridge, Massachusetts 02139

SEMI-ANNUAL TECHNICAL REPORT

June 1, 1971

Sponsored by

Advanced Research Projects Agency

ARPA Order No. 1579

Contract No. HO110376

Contract Period: 11/17/70-11/16/71

Project Officer: James J. Olsen
Twin Cities Mining
Research Center
Twin Cities, Minnesota
55111

Unclassified
Security Classification

3200.8 (Att 1 to Encl 1)
Mar 7, 66

DOCUMENT CONTROL DATA - R & D

(Security classification of title, body of abstract and indexing annotation must be entered when the overall report is classified)

1. ORIGINATING ACTIVITY (Corporate author)
Massachusetts Institute of Technology
Dept. of Earth and Planetary Sciences
Cambridge, Massachusetts 02139

2a. REPORT SECURITY CLASSIFICATION
Unclassified

2b. GROUP
N/A

3. REPORT TITLE

Mechanics of Crustal Earthquakes

4. DESCRIPTIVE NOTES (Type of report and inclusive dates)
Semiannual Technical Report

5. AUTHOR(S) (First name, middle initial, last name)

William F. Brace, Pierre-Yves F. Robin, and Don K. Riley

6. REPORT DATE	7a. TOTAL NO. OF PAGES	7b. NO OF REFS
June 1, 1971	43	30

8a. CONTRACT OR GRANT NO.	9a. ORIGINATOR'S REPORT NUMBER(S)
H0110376	
b. PROJECT NO. 1579	72809-1
c. Work Unit No. F53211	9b. OTHER REPORT NO(S) (Any other numbers that may be assigned this report)
d.	

10. DISTRIBUTION STATEMENT

Distribution of this document is unlimited.

11. SUPPLEMENTARY NOTES	12. SPONSORING MILITARY ACTIVITY
	Advanced Research Projects Agency Washington, D. C. 20301

13. ABSTRACT

Part I - The theory of stick-slip is developed, based on the concept of a static and dynamic coefficient of friction. The dynamic coefficient is assumed to be independent of displacement and to depend wholly on normal stress across the surface. It is also assumed to be velocity-independent. The theory predicts that the stress drop during stick-slip is independent of machine stiffness. The displacement during stick-slip is by contrast directly proportional to the machine compliance. Two series of experiments with different fault angles would serve to evaluate the dynamic coefficient of friction.

Part II - Frictional sliding on sawcuts and faults in laboratory samples of various silicate rocks is markedly temperature-dependent. At pressures from 1 to 5 kb, stick-slip gave way to stable sliding as temperature was increased 200° to 500° C. The particular temperature of transition to stable sliding varied with rock type.

DD FORM 1 NOV 65 1473

Unclassified
Security Classification

14. KEY WORDS	LINK A		LINK B		LINK C	
	ROLE	WT	ROLE	WT	ROLE	WT
Rock Mechanics						
Earthquakes						
Minerology						
Stick-slip						
Friction						
High Pressure Rock Properties						

INTRODUCTION

This report describes our technical findings and accomplishments during the first six-month period of the contract. The report is in two parts, which may eventually be published separately and are therefore treated as if they were independent. In Part I, the results of our analytical studies are presented. In Part II, we give the results of our measurements of friction at high temperature.

PART I

An analysis of stick-slip on rock surfaces in the laboratory

Pierre-Yves F. Robin

ABSTRACT

The theory of stick-slip is developed, based on the concept of a static and dynamic coefficient of friction. The dynamic coefficient is assumed to be independent of displacement and to depend wholly on normal stress across the surface. It is also assumed to be velocity-independent. The theory predicts that the stress drop during stick-slip is independent of machine stiffness. The displacement during stick-slip is by contrast directly proportional to the machine compliance. Two series of experiments with different fault angles would serve to evaluate the dynamic coefficient of friction.

INTRODUCTION

Stick-slip is a type of relative motion between two surfaces in contact, under the action of shear stresses. It is characterized by jerky movements, separated by intervals during which no significant relative displacement occurs. This effect has been studied in metals (1, 2, 3)

and, more recently, in rocks (4, 5, 6). Stick-slip in metals has usually been interpreted in terms of two coefficients of friction, one static and one dynamic. However, because the experimental systems used were dynamically complex, the problem of deducing the value of the dynamic coefficient of friction from the observed motion has not yet been solved (7). On rock surfaces, stick-slip has also been interpreted as the result of a dynamic coefficient of friction smaller than a static one (8). It is also possible, however, that stick-slip results from random variations of the average coefficient of friction as the two surfaces move by each other.

An understanding of this phenomenon is important to the geophysicist, because stick-slip is a possible mechanism for earthquakes (6, 9, 10). As Burridge and Knopoff (10) forcefully put it, "the nature of the friction during a shock determines the configuration of the system when it has finally come to rest. It is this final state that determines the conditions surrounding the next succeeding shock. Hence, if the demonstrations of the laboratory and numerical models are borne out in nature, it would seem likely that the nature of the friction on a fault surface determines the statistical properties of the earthquake shocks that are observed ...."

This paper analyses the dynamics of stick-slip for the experimental system which is most likely to provide data

pertinent to earthquake studies. The analysis shows how characteristics of friction may be obtained from experimental results. Available data (11) do not contradict the hypotheses proposed.

REPRESENTATION AND CHARACTERISTICS OF STICK-SLIP MOTION

In a typical experimental study of friction on rocks, a cylindrical specimen has a pre-existing cut at an angle with its axis. Jacketed, this specimen is submitted to a constant confining pressure p, and a load parallel to the axis of the cylinder is then applied. The displacement measured is the relative displacement, parallel to the axis, of two parts of the machine on either side of the specimen, usually sufficiently far from the actual cut to show no significant displacement during the stress drop. A typical record is shown on Figure 1(a). Such an experiment is often reported as Figure 1(b) (e.g. 6), obtained from Figure 1(a) by removing from the displacement the part which is due to the elastic compliance of the machine. Slopes of lines like F_1I_2 are the same as the slope corresponding to the elastic deformation of the whole specimen, except, perhaps, very close to I_2. It is concluded that, in general, no significant sliding occurs along the cut when the stress increases from F_1 to I_2. Hoskins *et al* (5), with an experimental system widely different from the one described here, and with a

Figure 1

(a)

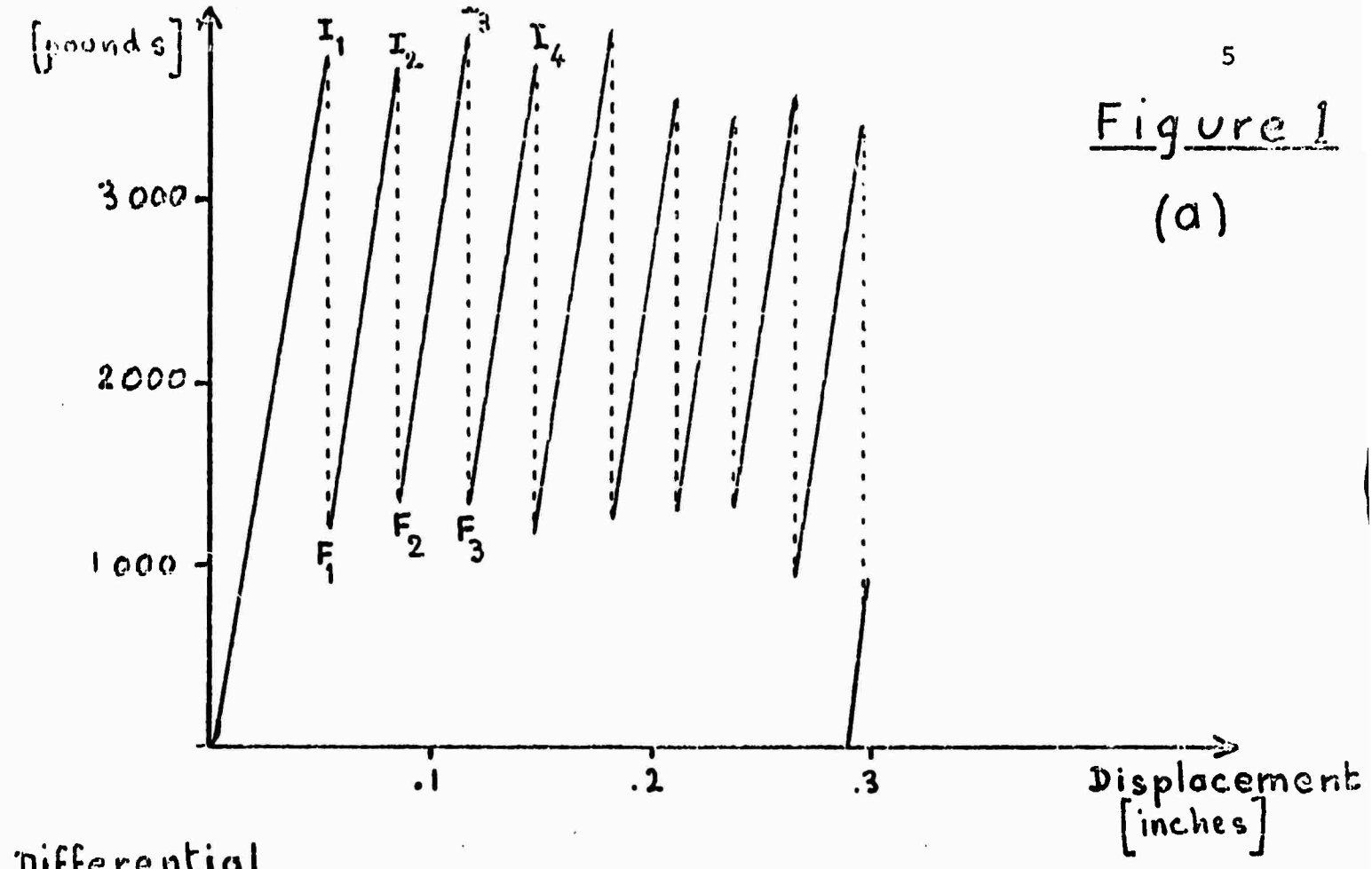
[pounds]
3000
2000
1000
I_1
I_2
I_3
I_4
F_1
F_2
F_3
.1
.2
.3
Displacement
[inches]

(b)

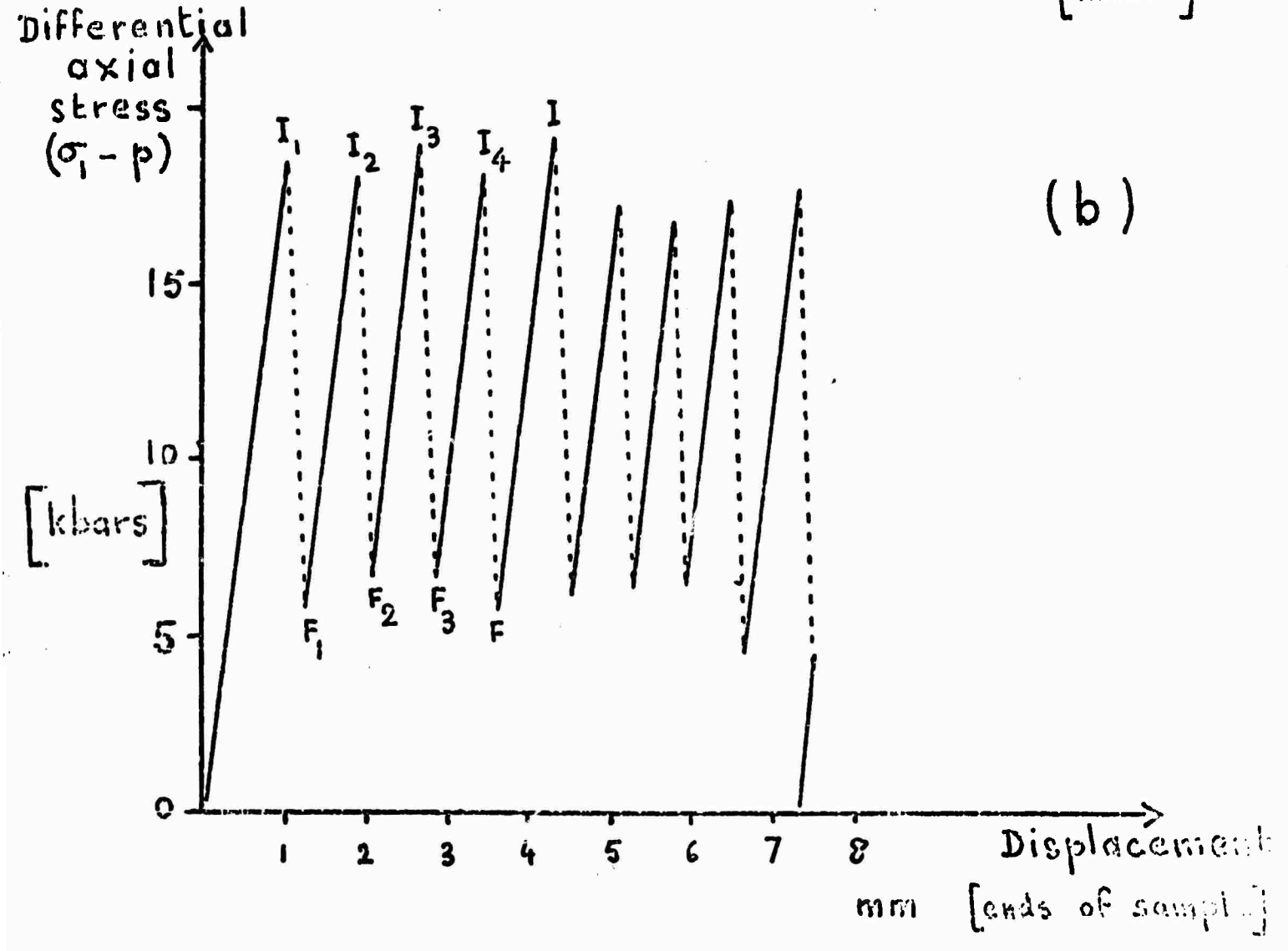
Differential
axial
stress
$(\sigma_1 - p)$
15
10
[kbars]
5
0
I_1
I_2
I_3
I_4
I
F_1
F_2
F_3
F
1
2
3
4
5
6
7
8
Displacement
mm
[ends of sampl

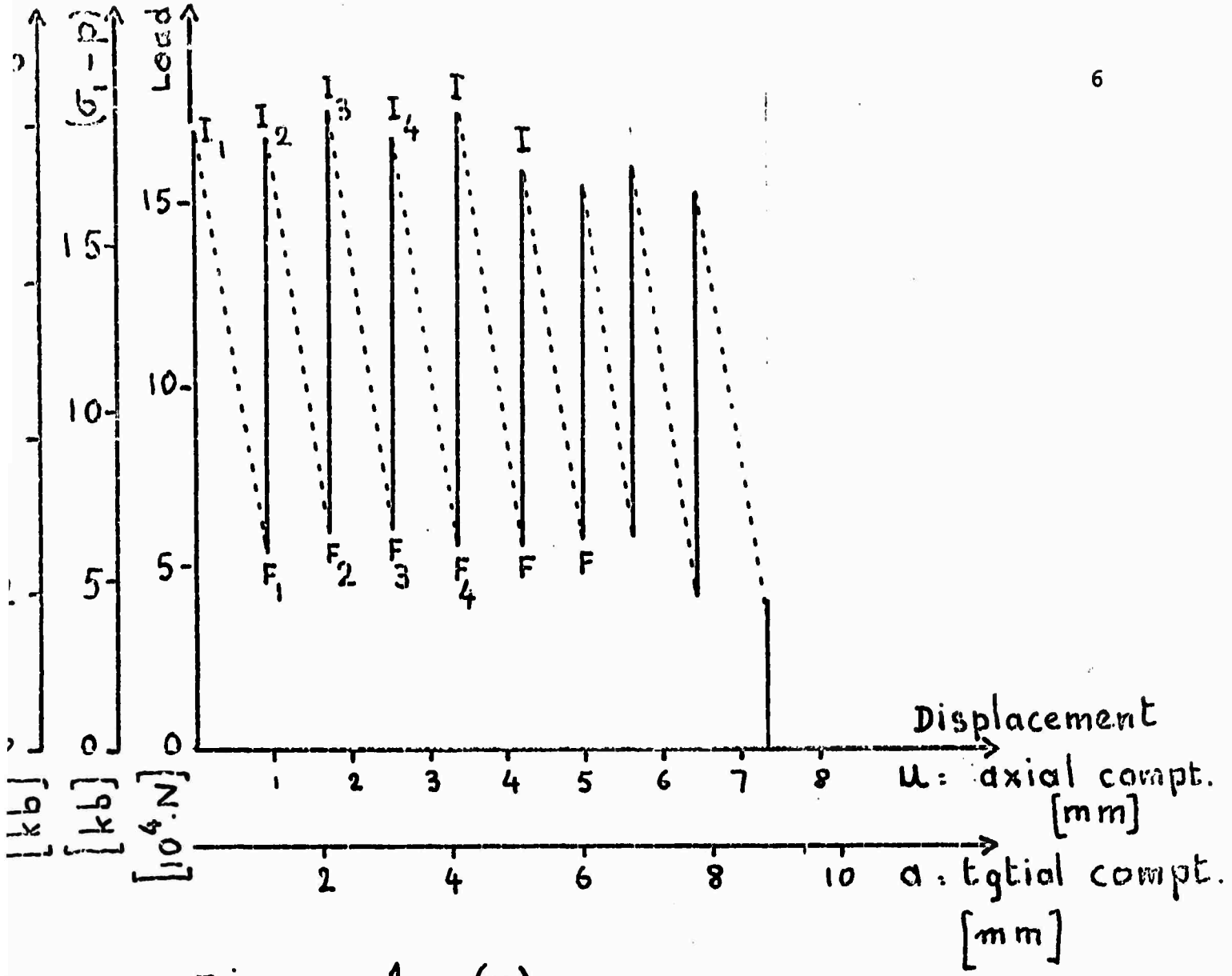

Figure 1 (c)

Various representations of a stick-slip experiment. Westerly Granite (sample diameter: 0.625 in; ground surface, at angle 0 = 30°; confining pressure: 4.59 kb). After Byerlee (11).

normal load never exceeding 70 bars, showed some movement along the surface, at constant value of stress, before the slip occurs. In general, however, we will assume that displacement only occurs during the stress drop.

If the angle of cut θ is defined as shown on Figure 4, differential stress (σ_1-p) and confining pressure p can be converted into normal and shear stresses by the following equations

$$\sigma_n = p + (\sigma_1 - p). \quad \mathrm{Sin}^2\theta \tag{1}$$

$$\tau = (\sigma_1 - p). \quad \mathrm{Sin}\ \theta. \quad \mathrm{Cos}\ \theta \tag{2}$$

Stick-slip experiments may then be reported as on Figure 1(c), where the displacement plotted is the relative displacement a parallel to the surface, or its axial equivalent u.

$$\Delta u = \Delta a. \quad \mathrm{Cos}\ \theta \tag{3}$$

Figure 1(c) can be considered as transformed from Figure 1(a) by subtracting the displacement due to the compliance of the "machine", where "the machine" is now understood to include the length of the specimen. Because, indeed, for the surface in motion, it is, to this point, immaterial whether the compliance is provided by steel, granite or Teflon, this representation is preferable. It may be pointed out also that the affine transformation from 1(a)

to 1(c) can be performed geometrically, without having to measure separately the various compliances involved. The displacement of the driving mechanism during the time of a stress drop can be neglected, and the slope of lines like I_1F_1 (in axial load vs. axial displacement coordinates) is therefore equal to the inverse of the compliance S of the "machine".

The shear stress at points like I_1 is the shear stress necessary to overcome friction. After a number of stress drops which depends on the confining pressure, some equilibrium is reached, and the stresses at points like I_3, I_4, etc. remain approximately constant, sometimes remarkably so (5, 6). Values of the stress drops are often quite regular; they are, typically, of the order of half the maximum stress.

THEORY

In this paragraph and the next, it is often easier to deal with differential axial load F and axial displacement u than with the shear stress τ and the displacement parallel to the friction surface a. As seen on Figure 1(c), the transformation involves only a change of scale along the axes, and the conversion factors are based entirely on the geometry of the system. In particular u (Eq. 3) designates the axial component of a, i.e. of the relative displacement

of two points immediately adjoining the cut and on either side of it. Also, the following quantities, having the dimension of a work, are equal:

$$F.du = A.\tau.da$$

where A is the surface area of contact.

Clearly, stick-slip requires that the resistance to shear, immediately after initiation of motion, would be smaller than before motion. If this were not the case, as an infinitesimal motion, du, causes a decrease dF = S.du in the force applied by the machine, further motion would then be resisted by friction, until the driving mechanism raises F again. Sliding on the surface would then be stable. Before exploring the various possibilities, it is useful to study the energy transformations during stick-slip. The argument given here is similar to the one given by Rabinowicz (7), but includes the seismic energy in the system.

Let E_I be the initial elastic stored in the machine, before slip occurs. During the stress drop, neglecting the very small amount of energy given by the driving mechanism, this energy is transformed into several terms:

$$E_I = E_H + E_P + K_K + E_C \qquad (4)$$

where E_H is the heat, or friction energy, generated on the surface;

E_P is the sum of the potential elastic energies of all parts of the system;

E_K is the sum of the kinetic energies of all parts of the system; E_K may include attenuation energy, i.e. heat generated, by vibrations, elsewhere than on the friction surface;

E_C is the work done against the confining pressure.

In general, when relative motion across the friction surface stops, not all parts of the system stop. The terms E_P and E_K of equation (4) can be redistributed into an elastic potential term for the final position E_F, and a seismic term E_S. E_S, like E_K, may include or transform into heat, generated elsewhere than on the friction surface. The energy equation becomes

$$E_I = E_H + E_F + E_S + E_C \tag{5}$$

Now, the origin of the axial displacement u can be taken at the position before motion, and u may be defined as positive as in Figure 1. The heat generated is then given by

$$E_H = \int_o^{\Omega} F \cdot dy \tag{6}$$

Because forces are taken as positive when corresponding to compressions, the compliance S of the machine is a negative quantity. It can be assumed constant over the range of the stress drop. Calling F_I the axial force on the surface at

equilibrium, before initiation of motion, the decrease in elastic energy is

$$E_I - E_F = \int_o^{\mu} (F_I + \frac{1}{S} y)dy + E_C \qquad (7)$$

Substituting (6) and (7) into (5) gives:

$$\int_o^{\mu} (F_I + \frac{1}{S} y - F)dy = E_S \qquad (8)$$

E_S, the energy dissipated seismically, is always positive. Therefore Equation (8) is expressed by the following inequality for the oriented surface areas of Figure 2:

$$A_1 + A_2 > 0 \qquad (8')$$

The possibility, mentioned earlier, that stick-slip would result from random variations of the average friction coefficient across the interface can be represented as on Figure 3(a). Several features of Figure 3(a) distinguish it from Figure 1(c) and make this theory difficult to reconcile with the observed phenomenon without further modification.

After a stress drop, the shear stress across the surface increases without displacement, along branches like F_1G_1, and this is similar to branches F_1I_1 in Figure 1(c). But stable sliding along branches like F_1I_1 would then occur, following the random friction curve. The stress levels at

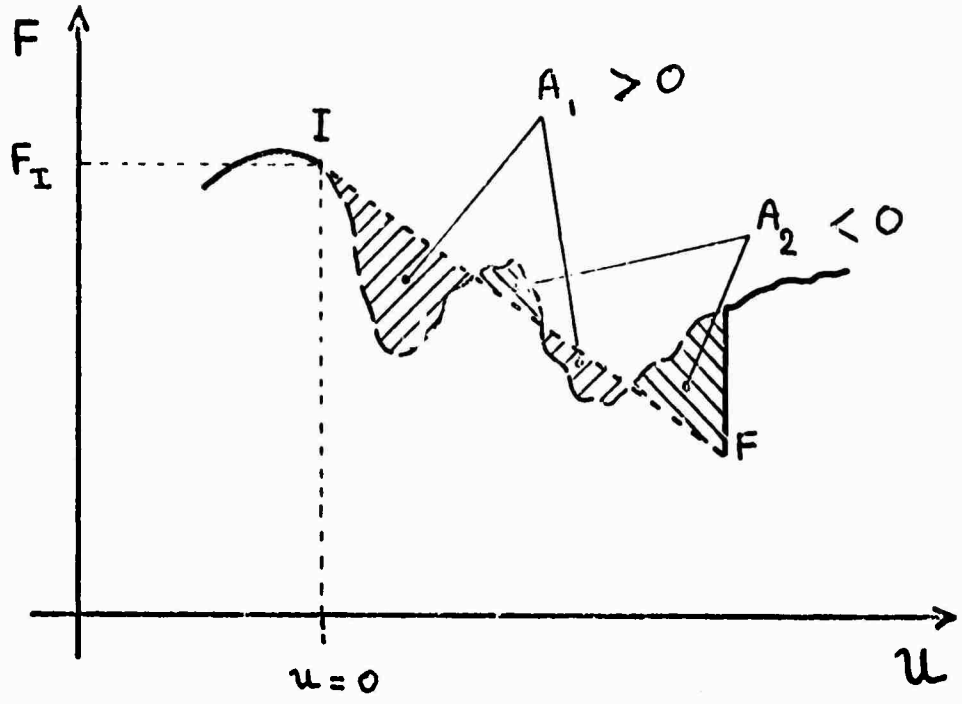

Figure 2 $A_1 + A_2 > 0$

Energy equation for stick-slip when friction varies with displacement.

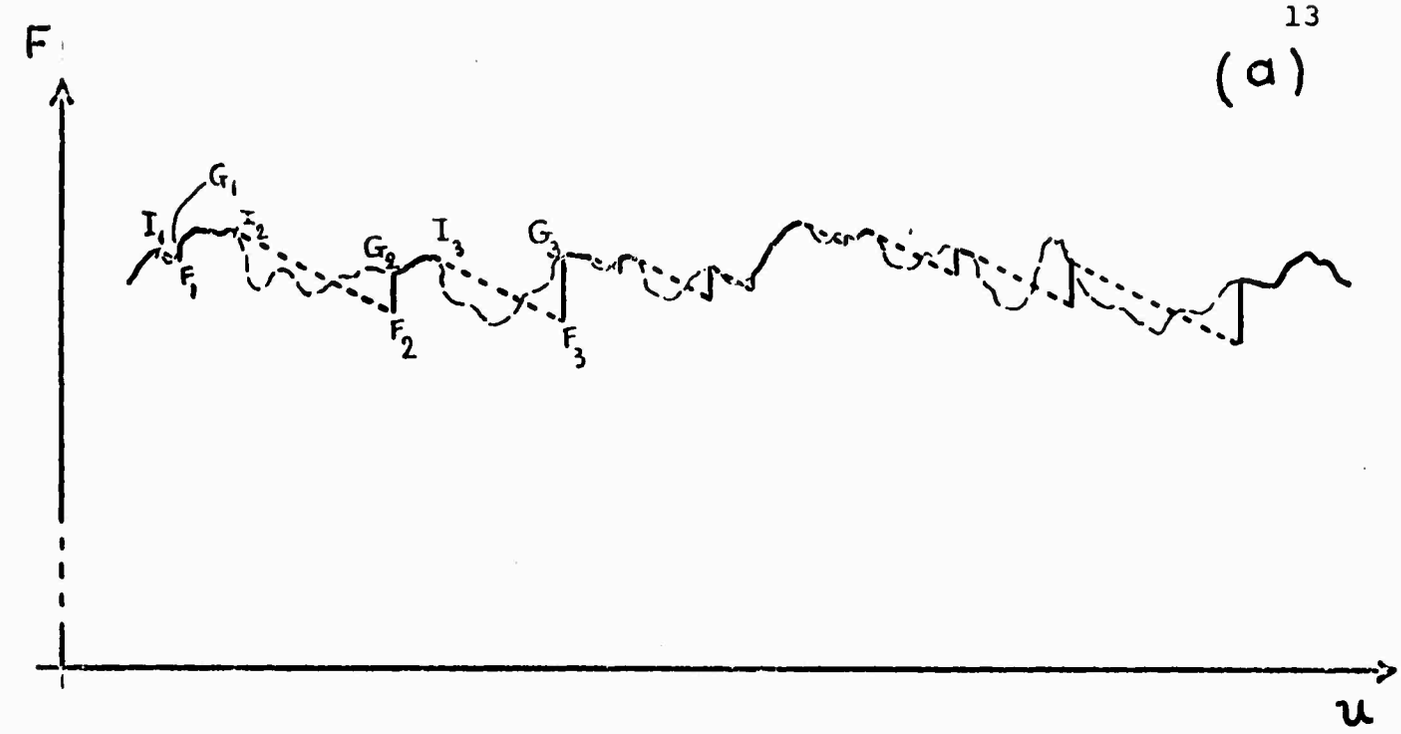

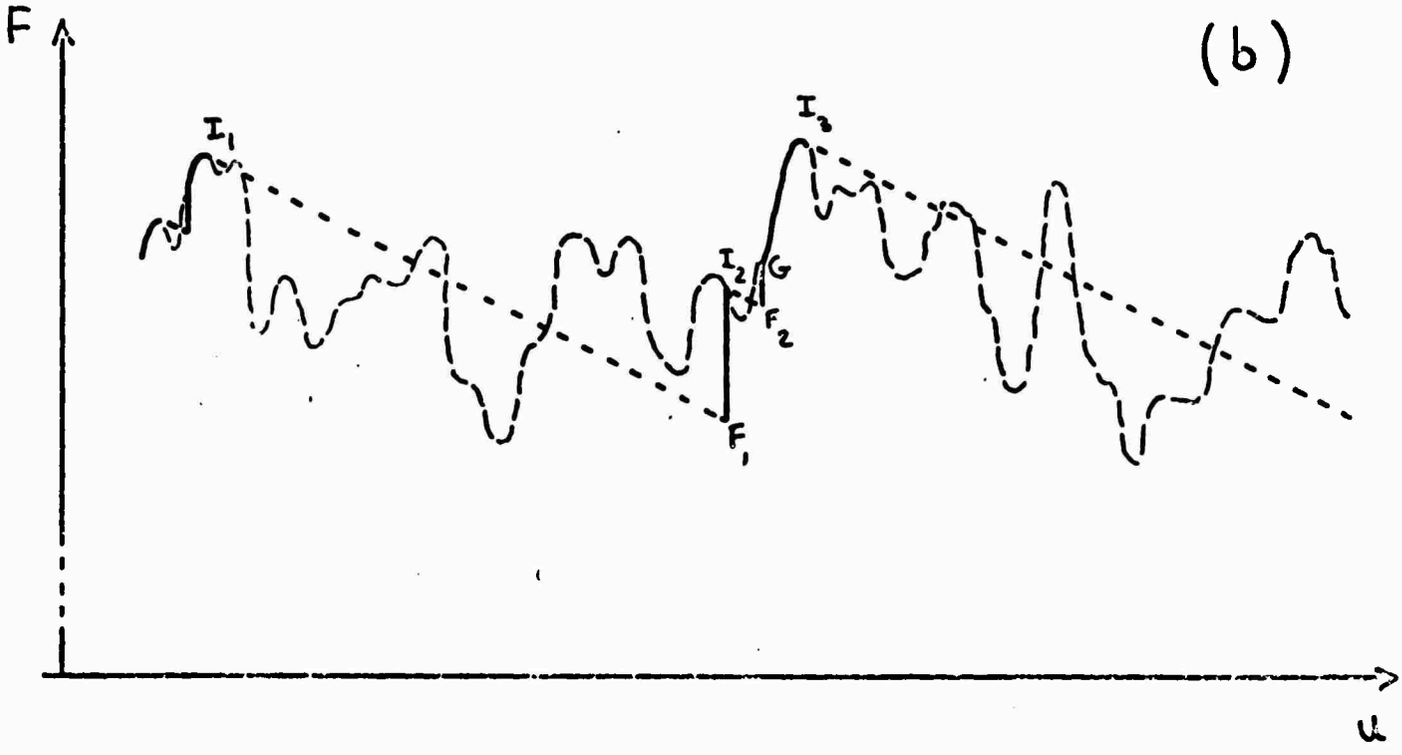

Figure 3

Irregular stick-slip, caused by variation of the resistance of friction with displacement.

point I or F would also be expected to show wider variations than the ones observed. Finally, a reduction of the compliance of the machine would be expected to cause stick-slip to disappear, ard this is not found by experiments (6). This model can account, however, in a rough qualitative way, for the observed increase in the amplitude of the stress drop with an increase in confining pressure. Figure 3(b) is similar to Figure 3(a), drawn for the same hypothetical interface, under a higher normal stress. The compliance of the machine, however, is approximately unchanged. The stress drops can be seen to be statistically higher than in the case of Figure 3(a). In spite of this, and because of the reasons given previously, irregular variation with displacement of the average friction as an explanation of stick-slip (Rabinowicz's irregular stick-slip, 7) is tentatively rejected here. The other possibility, accepted for metals, is to consider the existence of a dynamic coefficient of friction, smaller than the static coefficient of friction, without at first trying to explain the physical nature of this difference. A priori, many factors may influence this dynamic coefficient of friction. As suggested by its very appearance, the dynamic coefficient may depend on the velocity of relative displacement during the stress drop itself; or it may also depend on the amount of relative displacement since the beginning of the individual stress drop. The dynamic coefficient may also depend on the

total amount of displacement since the beginning of the experiment. It may be a function of the normal stress across the sliding surface, or a function of the orientation of the stress quadric with respect to the surface.

Before developing the model, for reasons of simplicity, the following assumptions will be made:

(1) The dynamic coefficient of friction is independent of the total amount of displacement since the beginning of the experiment. This may be justified by the fact that, after a few initial stress drops, stick-slip becomes a fairly stable phenomenon, as mentioned in Section II.

(2) The dynamic coefficient, like the static (e.g. 4, 5, 12), depends only on the normal stress across the surface, and does not otherwise depend on the orientation of the stress quadric. The law of static friction for many rocks can be expressed by a relation of the form (4, 5, 6, 12)

$$\tau = S_s + \mu_s \cdot \sigma_n \qquad (9)$$

where S_s and μ_s are constants. In the same way, dynamic friction is assumed to be of the form

$$\tau = S_d + \mu_d \cdot \sigma_n \qquad (10)$$

(3) μ_d is constant, i.e. independent of the amount of displacement during the individual stress drop,

or of the displacement velocity. It is not essential that μ_d reaches this constant value at the immediate initiation of motion, but it is assumed to have reached it during most of the motion. This assumption can only be justified, refined or discarded by the agreement or disagreement of predictions based on it with experimental results.

The development of the model is now a relatively simple matter.

DEVELOPMENT OF THE MODEL

A schematic diagram of the machine of the model is shown on Figure 4. The shear stress component on the surface is applied through a "column" of springs of varying characteristics (steel, rock, etc.). The surface area of friction, A, is assumed not to vary significantly during one single stress drop. Under the highest confining pressure, A may in fact vary by 3 or 4%. The confining pressure p is kept constant during the stress drop.

Immediately before initiation of motion the stress components near the surface are related by Equations (1) and (2); σ_n and τ are themselves related by Equation (9). Equations (1), (2) and (9) combine into

$$\sigma_{1,s} = p + \frac{S_s + \mu_s \cdot p}{\sin\theta(\cos\theta - \mu_s \sin\theta)} \qquad (11)$$

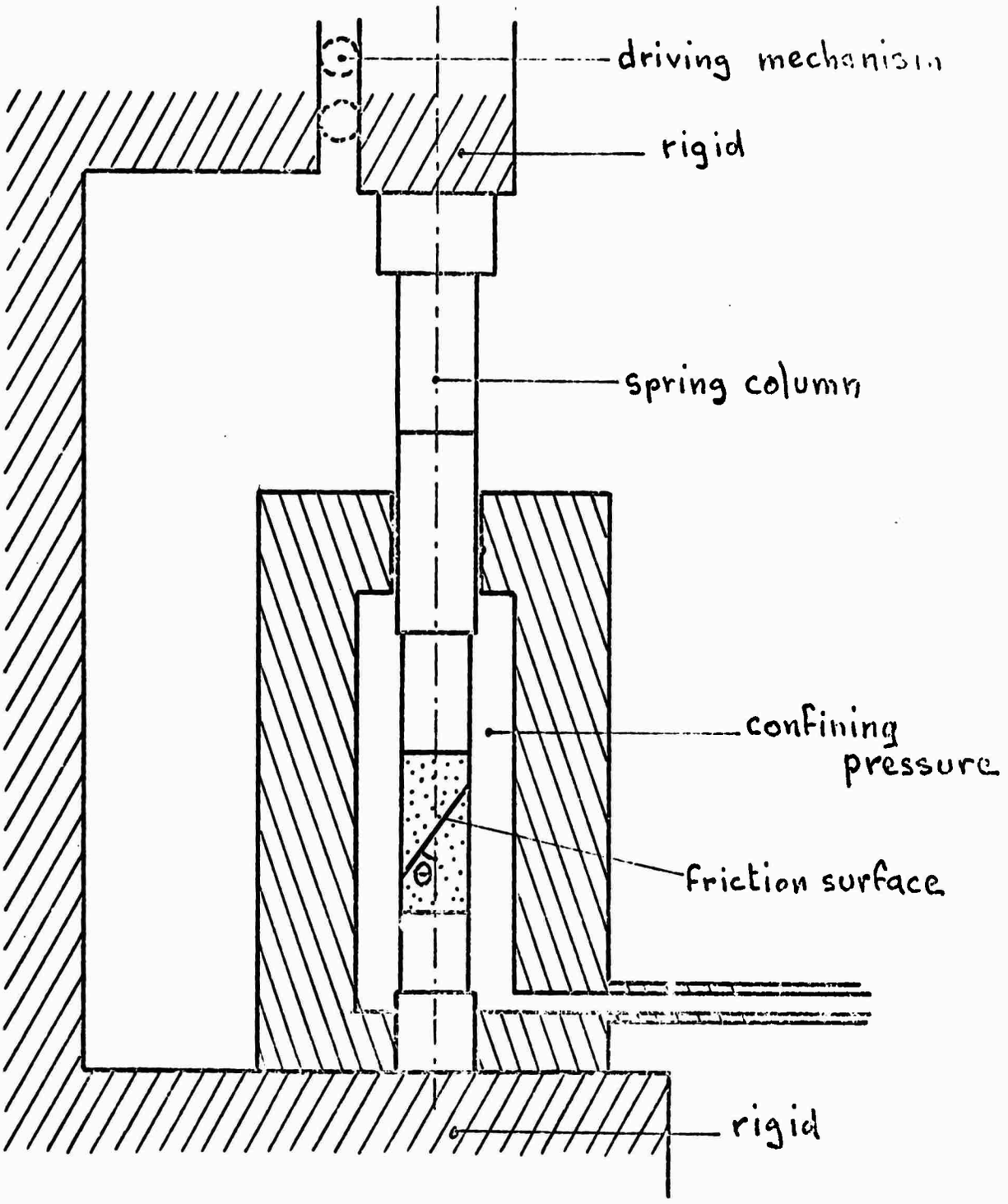

Figure 4

Sketch of a machine used to study stick-slip on rock surfaces with high normal pressures.

Consider now the state of stress during motion, in the immediate vicinity of the surface. The inertial forces due to lateral accelerations in the specimen are neglected. The minimum principal stresses are still $\sigma_1 = \sigma_2 = p$. The angle θ being unchanged, Equations (1) and (2) are still the transformation laws. When they are combined with Equation (10), the same algebra as in the static case leads to a similar equation:

$$\sigma_{1,d} = p + \frac{S_d + \mu_d \cdot p}{\sin\theta(\cos\theta - \mu_d \cdot \sin\theta)} \qquad (12)$$

To $\sigma_{1,s}$ and $\sigma_{1,d}$ correspond axial forces F_s, F_d, by the geometric relation $F = A \sin\theta \cdot \sigma_1$. The problem can now be expressed in the following manner: a spring column, along which mass and compliance are distributed non-uniformly, is compressed, in equilibrium, by a force F_s. The force is suddenly reduced to a lower value F_d. What is the amplitude of the first uniform motion of the end of the spring?

Figure 5 is another sketch of the spring column. The coordinate along it is x. The column is fixed rigidly at $x = 0$. The displacement of a point, $\mu(x, t)$, is a function of time. The specific mass per unit length is a function of position, $m(x)$, and is always positive. The specific compliance is also a function of position, $s(x)$. Because of our convention that compressions are positive and that displacements corresponding to stress drops are also positive, $s(x)$ is

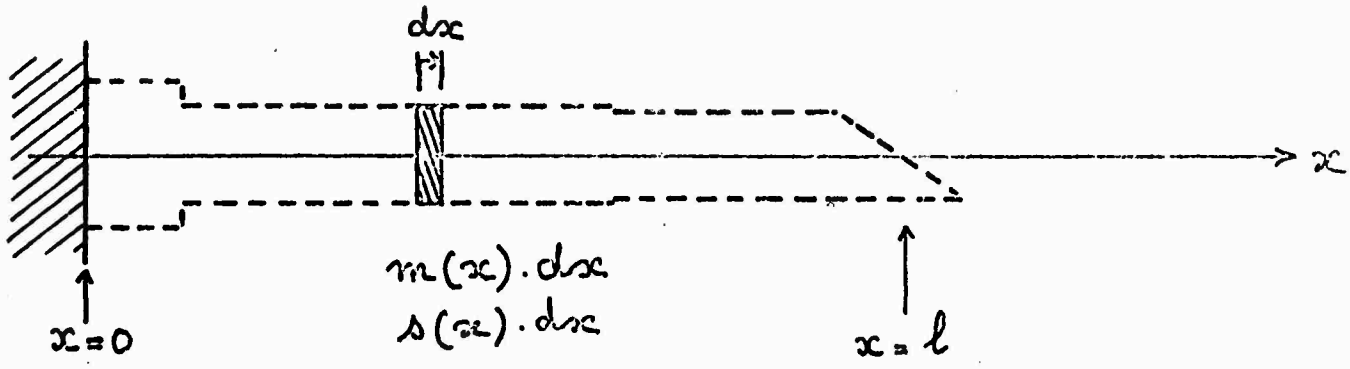

Figure 5

Diagram of the spring column.

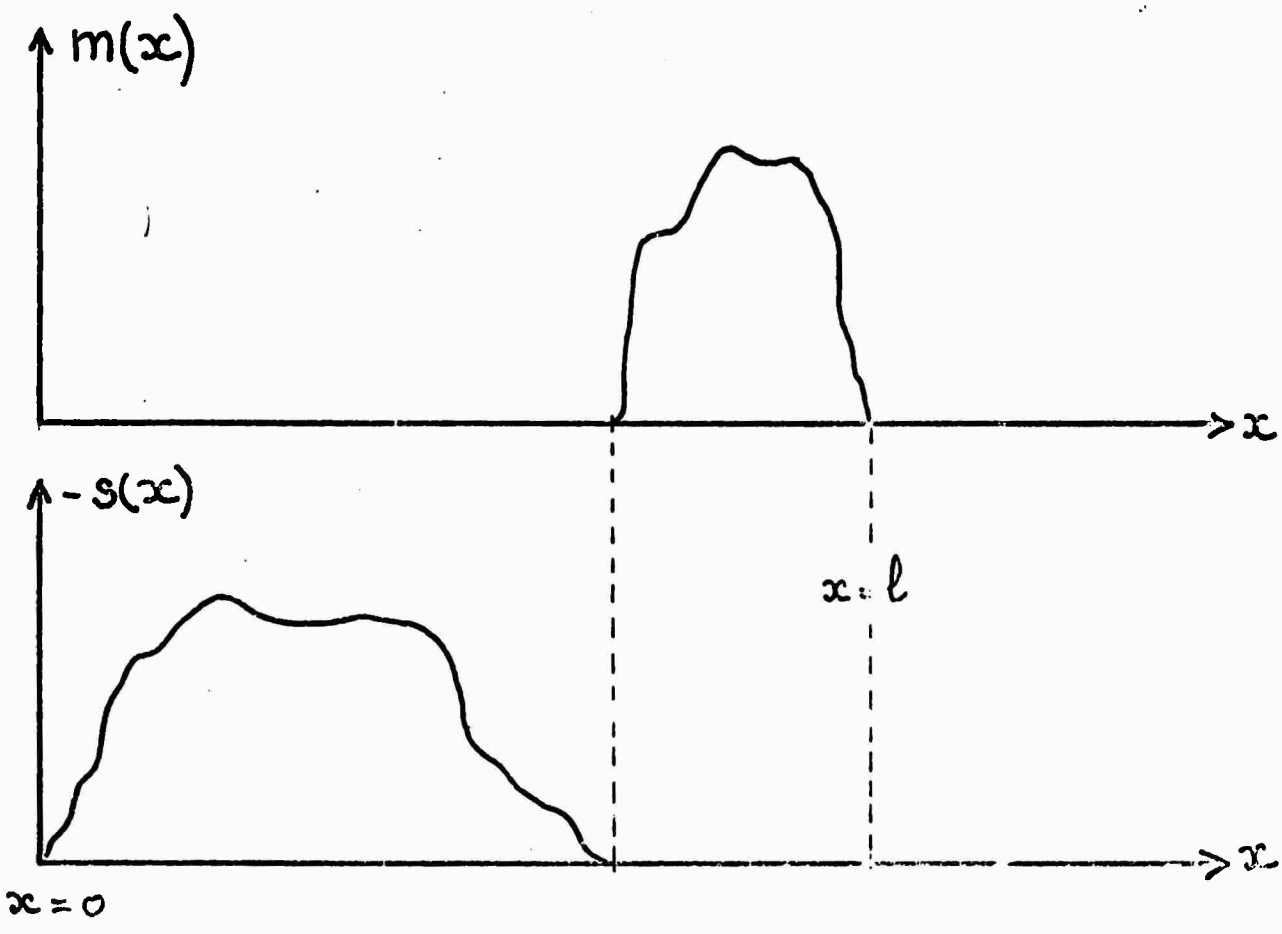

Figure 6

Distribution of mass and compliance. Case of a rigid mass at the end of a massless spring.

always negative; s(x) can be zero (rigid section), but cannot be infinite. The total compliance of the machine is given by:

$$\int_0^l s(x).dx = S, \text{ negative} \tag{13}$$

The origin of displacements u(x, t) may be taken as the position of each section immediately before slip. It can be shown that the equation of motion is:

$$\frac{\partial^2 u}{\partial t^2} + \frac{1}{m(x)} \cdot \frac{\partial}{\partial x} \left(\frac{1}{s(x)} \cdot \frac{\partial u}{\partial x}\right) = 0 \tag{14}$$

The initial conditions are that

$$\text{at } t = 0: \quad \begin{cases} u(o, t) = 0 \\ \dfrac{\partial u}{\partial t} = \dfrac{\partial^2 u}{\partial t^2} = 0 \quad \text{for any } x \\ \dfrac{1}{s(x)} \cdot \dfrac{\partial u}{\partial x} = 0 \text{ for any } x \end{cases} \tag{15}$$

The boundary conditions, when t > 0, are

$$\begin{cases} u(o, t) = 0 \\ \dfrac{1}{s(l)} \cdot \dfrac{\partial u(l,t)}{\partial x} = [F_d - F_s], \text{ for any } t \end{cases} \tag{16}$$

Let T be the time at which the velocity of the end of the spring comes to 0. At this time, the coefficient of friction resumes its static value and relative displacement stops. The axial component of the relative displacement

for the stress drop is thus u(1, T). In the general case, Equation (14) is not easy to solve and must be integrated numerically. However, if the mass and the compliance are distributed as in Figure 6, the problem becomes one of an intertial pendulum with a massless spring; Equation (14) may be solved directly (2, 7, 8). Instead it can also be noted that for such a distribution of mass and compliance no seismic energy remains in the system after the end of the motion. In such case, Equation (8) gives (see also Figure 7):

$$u(1, t) = 2[F_d - F_s].S \qquad (17)$$

The argument leading to Equation (8) also indicates that this is the maximum value of u(1, T) for a machine with a given total compliance S. In general

$$u(1, T) = K.S.[F_d - F_s] \qquad (17')$$

where $0 < K < 2$

K is a constant coefficient characteristic of the machine, as can be shown easily. If u_1 is a solution of Equation (14) for a value $[F_d - F_s]$ in Boundary Condition (16), $u_2 = \alpha\, u_1$ is a solution for a boundary value $\alpha[F_d - F_s]$. In particular, if $u_1(1, T)$, equal to $K_1.S.[F_d - F_s]$, is the displacement in the first case, the displacement in the second case is:

$$u_2(1, T) = \alpha.u_1(1, T) = \alpha.K_1.[F_d - F_s] = K_2.S\ \alpha[F_d - F_s].$$

Therefore $K_2 = K_1 = K$.

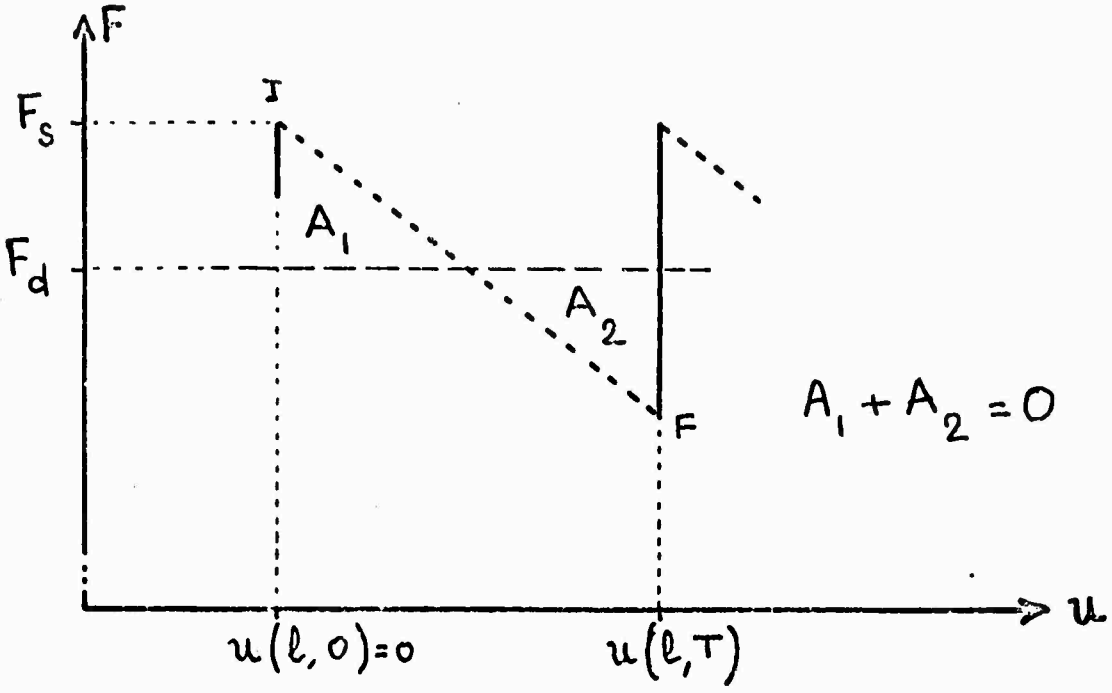

Figure 7

Stick-slip for a machine having a distribution of mass and compliance as in Figure 6.

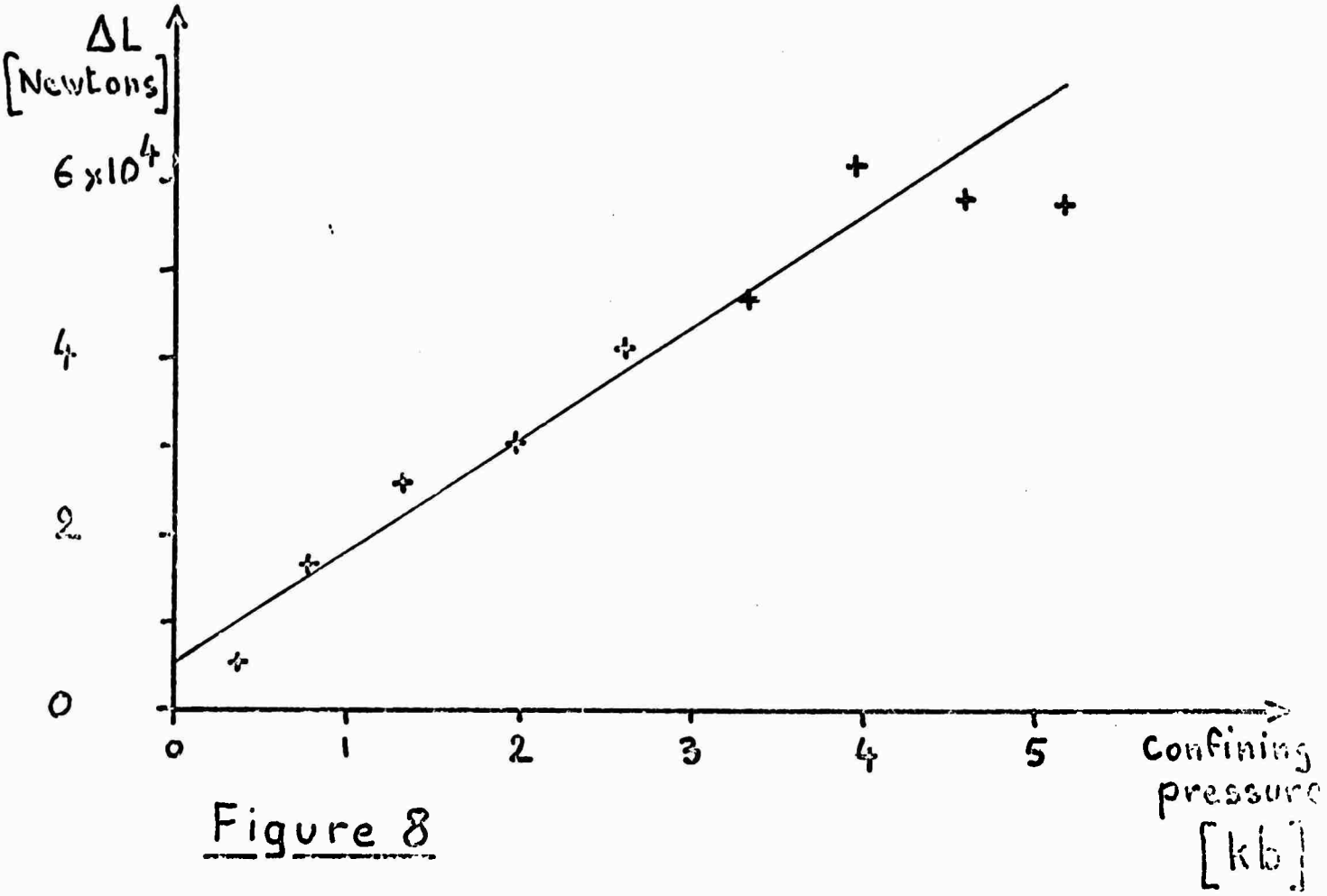

Figure 8

Increase of stress drop with confining pressure data from Byerlee (11). Corrected for the decrease in contact area.

The load drop is what is recorded directly in an experiment. In absolute value, it is equal to:

$$\Delta L = K[F_d - F_s]$$

Using Equations (11) and (12), it is:

$$\Delta L = K A\left[\frac{S_d}{\cos\theta - \mu_d.\sin\theta} - \frac{S_s}{\cos\theta - \mu_s.\sin\theta} + p\left(\frac{\mu_d}{\cos\theta - \mu_d.\sin\theta} - \frac{\mu_s}{\cos\theta - \mu_s.\sin\theta}\right)\right] \quad (18)$$

The load drop is thus found to be independent of the compliance S of the machine. This was found experimentally by Byerlee and Brace (6). Curves obtained by Byerlee (11) for friction of Westerly granite (with $\theta = 30°$) show that ΔL does increase linearly with confining pressure as predicted by Equation (18).

The quantities S_s and S_d are readily obtained experimentally, and have been obtained in particular for Westerly granite (12). The only unknowns in Equation (18) are therefore K, S_d and μ_d. The slope r of the line in Figure 8 gives the following equation:

$$r = K A\left(\frac{\mu_d}{\cos\theta - \mu_d.\sin\theta} - \frac{\mu_s}{\cos\theta - \mu_s.\sin\theta}\right) \quad (19)$$

or, numerically:

$$1.28(cm^2) = 7.92\ K\left(\frac{\mu_d}{1.733 - \mu_d} - 0.53\right)(cm^2) \quad (19')$$

Another series of experiments, with a different angle θ', would give another equation similar to (19). The two equations would then be sufficient to determine K and μ_d. The intersection of the two lines (as in Figure 8) with the ordinate axis, $p = 0$, should both give the same value of S_d. There is, however, a large degree of uncertainty for these intersections.

REFERENCES

1. F.P. Bowden and L. Leben (1939), Proc. Roy. Soc., A169, 371.

2. F.P. Bowden and D. Tabor (1950), The Friction and Lubrication of Solids, Oxford, Clarendon Press, p. 105 and ff.

3. F. Morgan, M. Muskat and D.W. Reed (1941), Friction phenomena and the stick-slip process, J. of Appl. Phys., 12, 743.

4. J.C. Jaeger (1959), The frictional properties of joints in rocks, Geofis. pura appl., 43, 148.

5. E.R. Hoskins, J.C. Jaeger and K.J. Rosengren (1968), A medium scale direct friction experiment, Int. J. Rock Mech. Min. Sci., 5, 143.

6. J.D. Byerlee and W.F. Brace (1968), Stick-slip, stable sliding, and earthquake: Effect of rock type, pressure, strain rate, and stiffness, J. Geophys. Res., 73, 6031.

7. E. Rabinowicz (1965), Friction and Wear of Materials, J. Wiley & Sons, p. 94 and ff.

8. J.C. Jaeger and N.G.W. Cook (1969), Fundamentals of Rock Mechanics, Methuen, p. 61 and ff.

9. F. Press and W.F. Brace (1966), Earthquake prediction Science, 152, 1575.

10. R. Burridge and L. Knopoff (1967), Model and theoretical seismicity, Bull. Seismol. Soc. Am., 57, 341.

11. J.D. Byerlee (1965), Stress-displacement curves of friction on surfaces of Westerly granite, unpublished results.

12. J.D. Byerlee (1967), Frictional characteristics of granite under confining pressure, J. Geophys. Res., 72, 3639.

13. F.P. Bowden and D. Tabor (1964), The Friction and Lubrication of Solids, Part II, Clarendon Press, Chap. XV.

PART II

Experimental studies of high temperature friction

W.F. Brace and D.K. Riley

ABSTRACT

Frictional sliding on sawcuts and faults in laboratory samples of various silicate rocks is markedly temperature-dependent. At pressures from 1 to 5 kb, stick-slip gave way to stable sliding as temperature was increased 200° to 500°C. The particular temperature of transition to stable sliding varied with rock type.

Several field and laboratory observations suggest that earthquakes result from a large-scale form of stick-slip (5). For one thing, unstable (stick-slip and earthquake-producing) and stable (fault creep and stable sliding) motion have been found both in the field and in laboratory experiments on rocks under high pressure. For another, the same mineralogic controls on stability have been noted in field and laboratory. For example, minute amounts of serpentine in a dunite produced stable sliding (6); fault creep in California seems restricted to areas where the San

9. F. Press and W.F. Brace (1966), Earthquake prediction Science, 152, 1575.

10. R. Burridge and L. Knopoff (1967), Model and theoretical seismicity, Bull. Seismol. Soc. Am., 57 341.

11. J.D. Byerlee (1965), Stress-displacement curves of friction on surfaces of Westerly granite, unpublished results.

12. J.D. Byerlee (1967), Frictional characteristics of granite under confining pressure, J. Geophys. Res., 72, 3639.

13. F.P. Bowden and D. Tabor (1964), The Friction and Lubrication of Solids, Part II, Clarendon Press, Chap. XV.

PART II

Experimental studies of high temperature friction

W.F. Brace and D.K. Riley

ABSTRACT

Frictional sliding on sawcuts and faults in laboratory samples of various silicate rocks is markedly temperature-dependent. At pressures from 1 to 5 kb, stick-slip gave way to stable sliding as temperature was increased 200° to 500°C. The particular temperature of transition to stable sliding varied with rock type.

Several field and laboratory observations suggest that earthquakes result from a large-scale form of stick-slip (5). For one thing, unstable (stick-slip and earthquake-producing) and stable (fault creep and stable sliding) motion have been found both in the field and in laboratory experiments on rocks under high pressure. For another, the same mineralogic controls on stability have been noted in field and laboratory. For example, minute amounts of serpentine in a dunite produced stable sliding (6); fault creep in California seems restricted to areas where the San

Andreas fault system cuts serpentine-bearing rocks of the Franciscan series (7).

How can the disappearance of earthquakes at shallow depths be explained on the basis of laboratory studies? Three possibilities are apparent: a mineralogic change with depth, existence at depth of certain pore pressure conditions known to stabilize sliding in rocks (8), and temperature increase. The last is the least understood. Stable sliding at high temperature is suggested by a few observations of stable faulting at high temperature (9) and by somewhat ambiguous results with powders deformed between rotating anvils (10).

There are relatively few laboratory studies of rock fracture at high temperature and pressure (11) and practically none of frictional sliding. The biggest experimental difficulty, particularly for sliding, is jacket design. The jacket, required in a triaxial experiment to exclude the gas pressure medium from the rock sample, is typically metal foil. The foil ruptures easily at any strain discontinuity such as a fault. Our procedure was to retain the thin foil, but to add a sleeve of graphite between rock sample and foil (Figure 1). The sharp offset at the fault is smeared out in the soft graphite, and appreciable motion on the fault is tolerated before the foil ruptures. This simple modification in jacket design enabled us to use otherwise standard experimental procedure

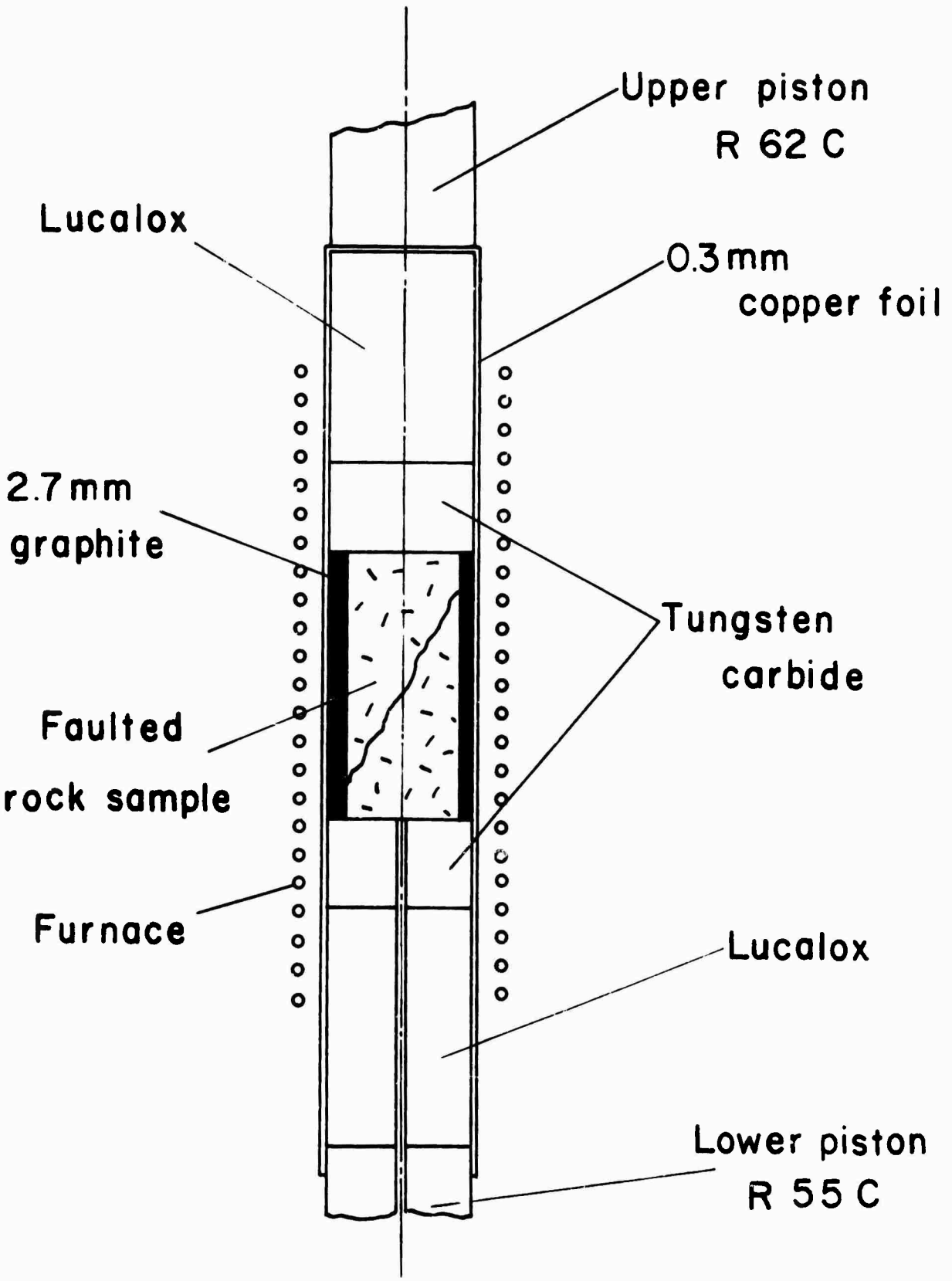
Upper piston
R 62 C
Lucalox
0.3mm
copper foil
2.7mm
graphite
Tungsten
carbide
Faulted
rock sample
Furnace
Lucalox
Lower piston
R 55 C

FIG. 1

for high temperature deformation study, to obtain the first detailed picture of the effects of temperature on friction of rocks.

The rock sample was a precisely ground cylinder 16 mm in diameter by 35 mm long. Sawcut, if present, was located midway between the ends and made an angle of 30° to the cylinder axis. Graphite sleeve was 1.3 mm thick, the annealed seamless copper foil, 0.32 mm thick.

An extensive series of experiments was conducted at room temperature to determine any possible stabilizing effect of the graphite-copper jacket. The results (Figure 2) revealed that a stabilizing effect on sliding existed only below 2 kb pressure. This took the form of lowering the amplitude of stick-slip to nearly zero. The shearing stress to cause frictional sliding increased about 10 percent compared with an experiment at the same pressure, using a 3 mm thick polyurethane jacket. Because of these effects, most experiments here were conducted at or above 2 kb pressure where room temperature experiments using copper-graphite were nearly identical with those using polyurethane. In any event, stabilizing effects present at room temperature probably would not be important at high temperature because of increased ductility of the copper.

Our apparatus resembled in a general way that described on page 46 of Reference 9. It was internally heated, with low friction O-ring seals. Stiffness of the loading system was

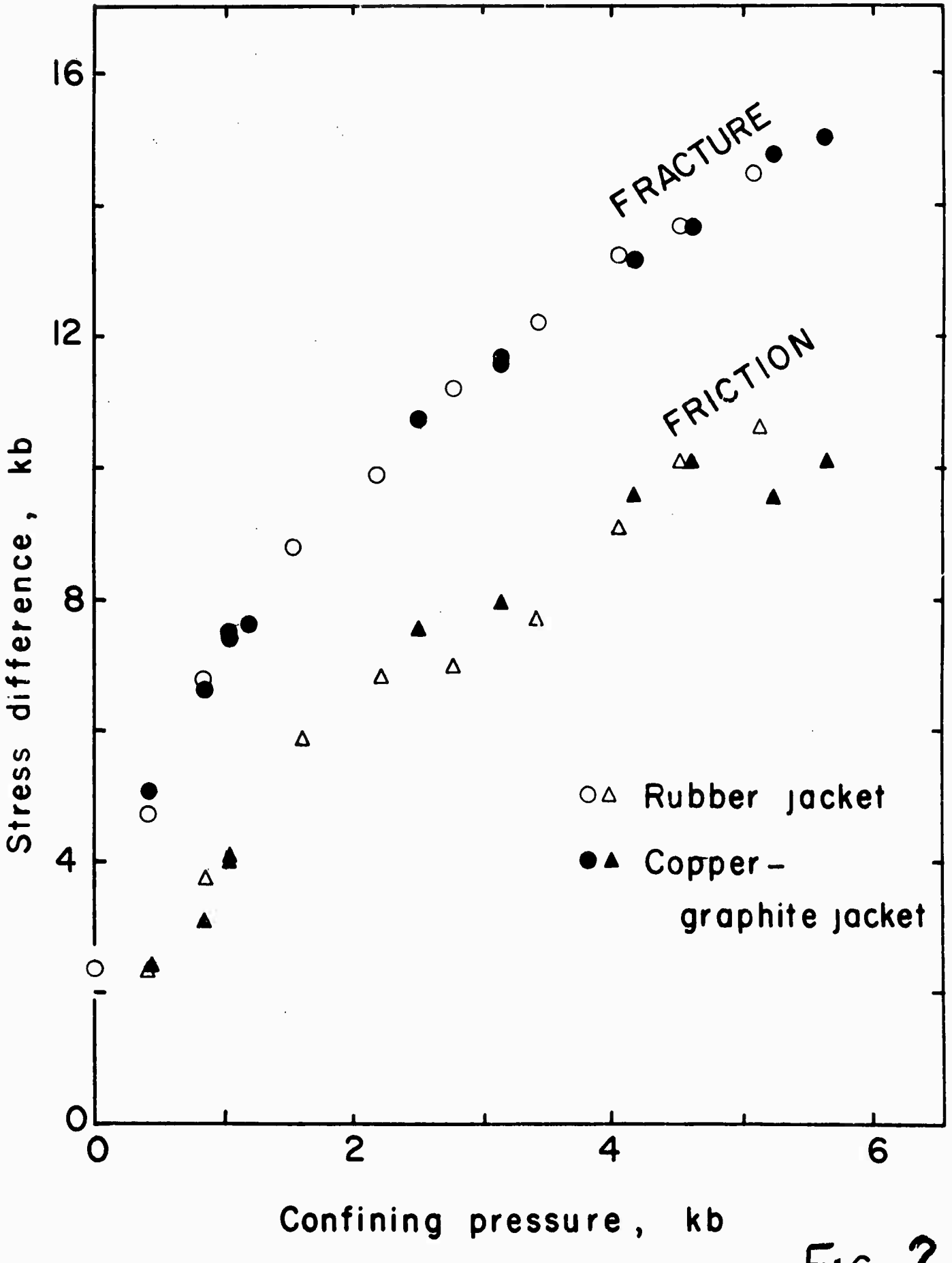
16
12
8
4
0
0
2
4
6
Stress difference, kb
Confining pressure, kb
FRACTURE
FRICTION
Rubber jacket
Copper-graphite jacket

FIG. 2

about 10^5 kg/cm. Pressure was known to 1 percent, temperature to about 10°. Strain rate was calculated from the rate of advance of the screw-driven piston.

Frictional sliding was studied in triaxial experiments in which the cylindrical sample contained a fault or sawcut (12). The fault was formed by loading an initially intact sample to failure; the sawcut was made in the sample at an angle (30°) close to that of typical faults (26-32°).

Of our two types of experiment, with sawcut and with fault, presumably the latter more nearly resembles actual faults. Sawcuts are flat and have a finely ground surface; faults have abundant gouge and the surface irregularity one normally associates with actual faults. Unfortunately a 'fault' experiment is more difficult and the results often more ambiguous than a 'sawcut' experiment. For example, each laboratory fault differs in detail; sawcuts are nearly identical; as a result, data from faulted samples shows greater scatter than that from sawcuts. For exploratory work, results from sawcuts are probably valid; Byerlee (13) found for granite only minor differences in friction between sawcuts and faults once some motion had occurred. Most of the results reported here are for sawcuts.

We studied frictional sliding in Westerly granite and San Marcos gabbro (14) at pressures to 5 kb, temperatures to 525°C, strain rates from 10^{-4} to 10^{-6}sec^{-1}. The samples were vented to the atmosphere through a hollow piston, so that presumably pore pressure was nearly zero.

The results for both rocks are shown in Table 1. In the first column, W refers to the granite and SM refers to gabbro. The displacement in the fourth column is displacement at pressure and temperature on the fault. In all runs the sample was heated at temperature for one hour, and the strain rate was 10^{-5} per second unless otherwise noted.

Results are shown in Figure 2 for sawcuts in granite. Apparently high temperature had a strong stabilizing effect on stick-slip; large amplitude stick-slip at low temperature (the 22° curve in Figure 3) gave way to stable sliding as temperature is increased (the 306° curve in Figure 3). Results at higher pressure were similar. No change in character of the sliding was evident over the 3 mm or so of sliding motion, which was the limit imposed by the apparatus. Neither strain rate nor heating procedure appeared to affect behavior such as shown in Figure 3. Samples were run at 10^{-4} to 10^{-6} sec^{-1} strain rate, were heated at pressure for 1 to 25 hours, with and without vacuum (10^{-2} Torr), and were heated and then run at room temperature.

Results for faults in gabbro are shown in Figure 4; these are also typical for granite. The faults were formed in the samples at 0.5 to 1 kb pressure and room temperature. Pressure and temperature were then raised to the conditions of the friction experiment. The marked effect of high

TABLE 1

High Temperature Friction

Expt.	P kb	T °C	Displ. mm	σ_D kb	Motion	Remarks
W-1-S	2.08	470	2.75	2.65	STA	$\dot{\varepsilon} = 10^{-4}$/sec
W-2-S	2.09	303	2.40	4.6	STA	$\dot{\varepsilon} = 10^{-4}$/sec
W-4-S	4.00	293	1.50	8.5	STK	Vac.htg.12 h @ 140°C
W-5-S	1.00	303	2.1	3.2	STA	$\dot{\varepsilon}$ ranged from 10^{-4} to 10^{-6}/sec
W-6-S	4.03	438	1.4	4.8	STA	
W-7-S	1.99	305	1.4	5.3	STA	25 hr.htg.at 2 kb, 300°C
W-7'-S	3.05	305	0.8	7.9	STA	
W-9-S	2.00	191	1.2	5.5	STA	
W-9'-S	4.00	197	1.0	9.1	STK	
W-10-F	4.04	439	1.5	11.3	STA	
W-11-F	4.00	260	3.7	11.7	STK	$\dot{\varepsilon} = 10^{-4}$/sec
SM-12-F	4.00	398	1.5	11.0	STA	$\dot{\varepsilon} = 10^{-4}$/sec;4 hrs. htg. @ 400°C
SM-13-F	5.00	197	4.3	11.5	STK	
SM-14-F	4.00	140	2.70	11.0	STK	$\dot{\varepsilon} = 10^{-4}$/sec
W-15-F	1.92	527	2.30	6.5	STA	
W-16-5	1.91	140	1.0	3.0	STK	
W-16'-5	1.91	203	0.8	3.7	STK	
SM-17-F	4.04	512	2.8	9.3	STA	
SM-18-F	4.13	100	2.0	11.5	STK	
W-19-F	5.05	403	3.2	13.9	STA	
W-20-F	6.11	405	1.6	14.9	STA	
W-21-F	4.95	350	1.5	12.3	STK	
W-22-F	3.00	390	1.5	7.8	STA	
W-25-F	3.52	206	2.2	11.5	STK	
W-26-F	5.02	512	2.0	13.1	STA	
SM-27-F	3.50	355	2.6	8.3	STA	
SM-28-F	3.00	103	2.0	9.0	STK	
SM-29-F	4.50	306	3.1	9.6	STA	

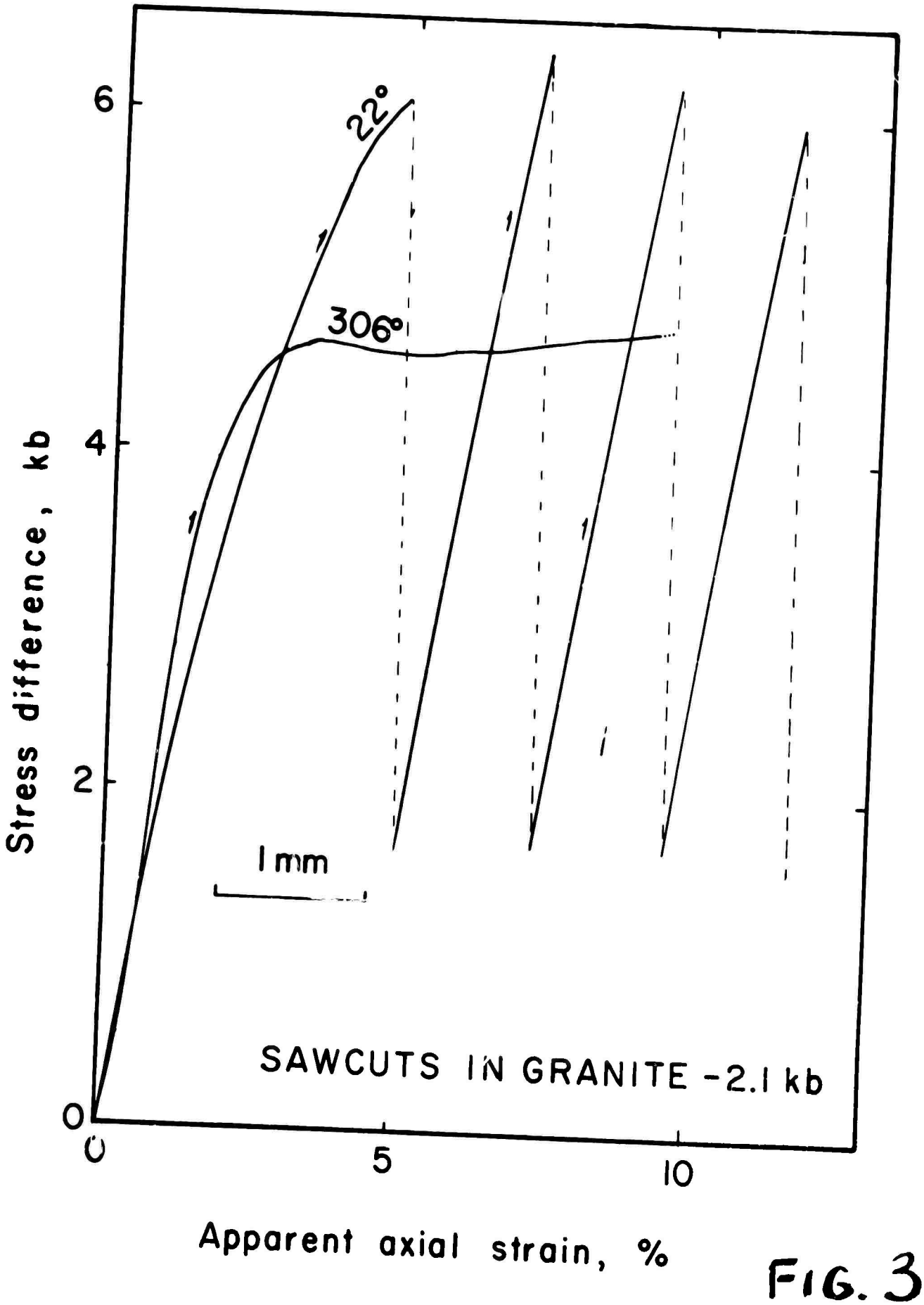
22°
306°
1
1
1
1
1
1 mm
SAWCUTS IN GRANITE -2.1 kb
Stress difference, kb
Apparent axial strain, %
0
2
4
6
0
5
10

FIG. 3

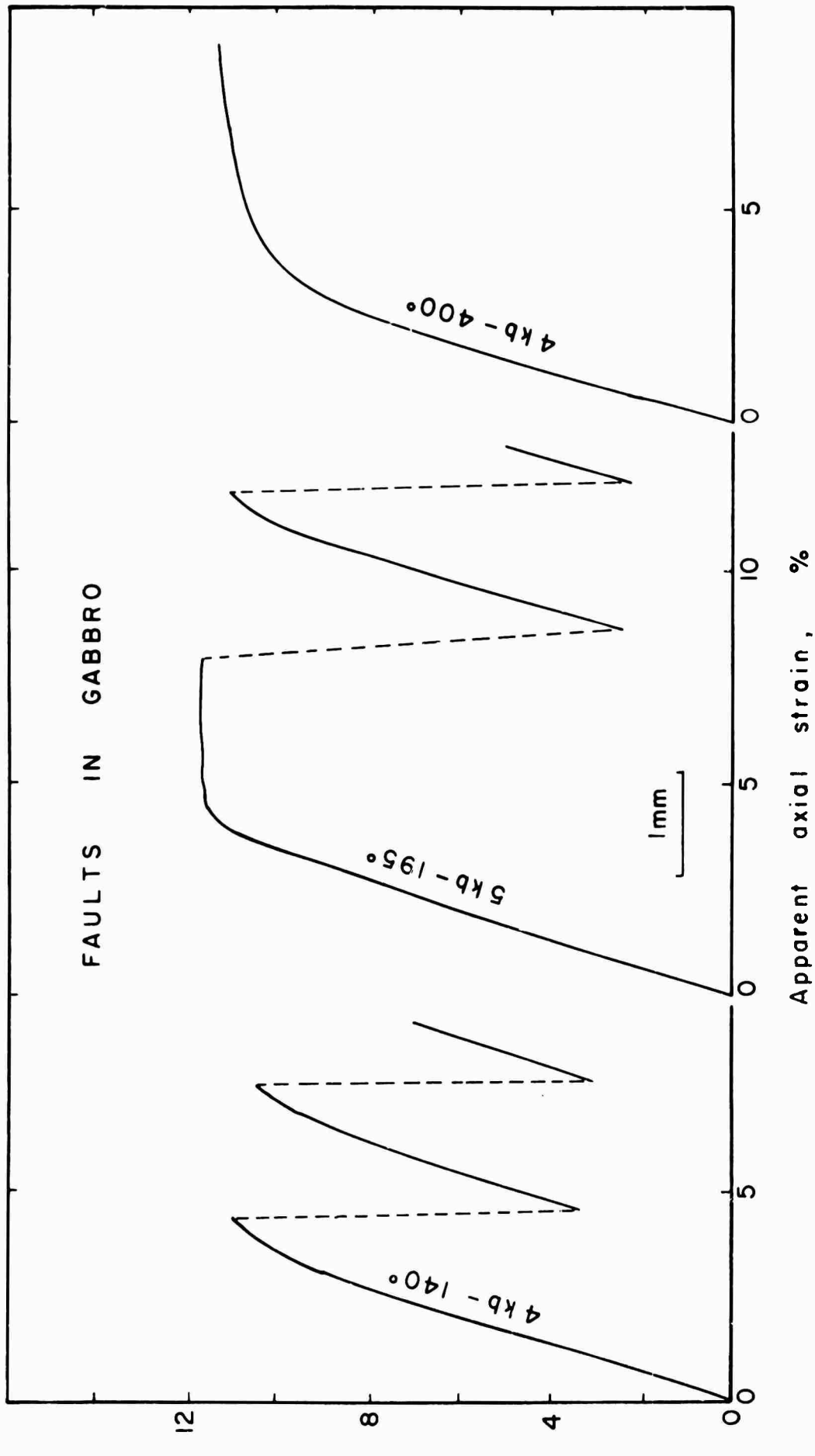
FAULTS IN GABBRO
4 kb - 140°
5 kb - 195°
4 kb - 400°
1mm
Stress difference, kb
Apparent axial strain, %
0
4
8
12
0
5
10
5
0
5
0

FIG. 4

temperature is again evident, although the transition between stick-slip and stable sliding appears less sharp than for sawcuts. In other words, there appears a significant range of temperature over which stick-slip was preceded by some stable sliding. It is not certain that even at the highest temperature stick-slip would not have occurred had there been additional displacement.

Results for both sawcuts and faults are shown in Figure 5, in which stick-slip (open figure) or stable sliding (closed figure) is indicated. Where appreciable stable sliding preceded the stick-slip, this is designated by a half-closed figure.

Several features are evident in Figure 5. First, sliding on granite sawcuts has a well-defined field of stability; thus, the sliding was stable at high temperature and low pressure, and unstable at high pressure and low temperature. Second, the field boundary for the sawcuts is very sharp; within about 100°C large amplitude stick-slip gave way to stable sliding. Third, the results for the faults in granite, although very limited in number, are at least consistent with results for the sawcuts; the transition from unstable to stable may be more gradual for faults than sawcuts at the pressures of these tests. Finally, the field boundary may be different for gabbro and granite with stick-slip disappearing at lower temperature for gabbro.

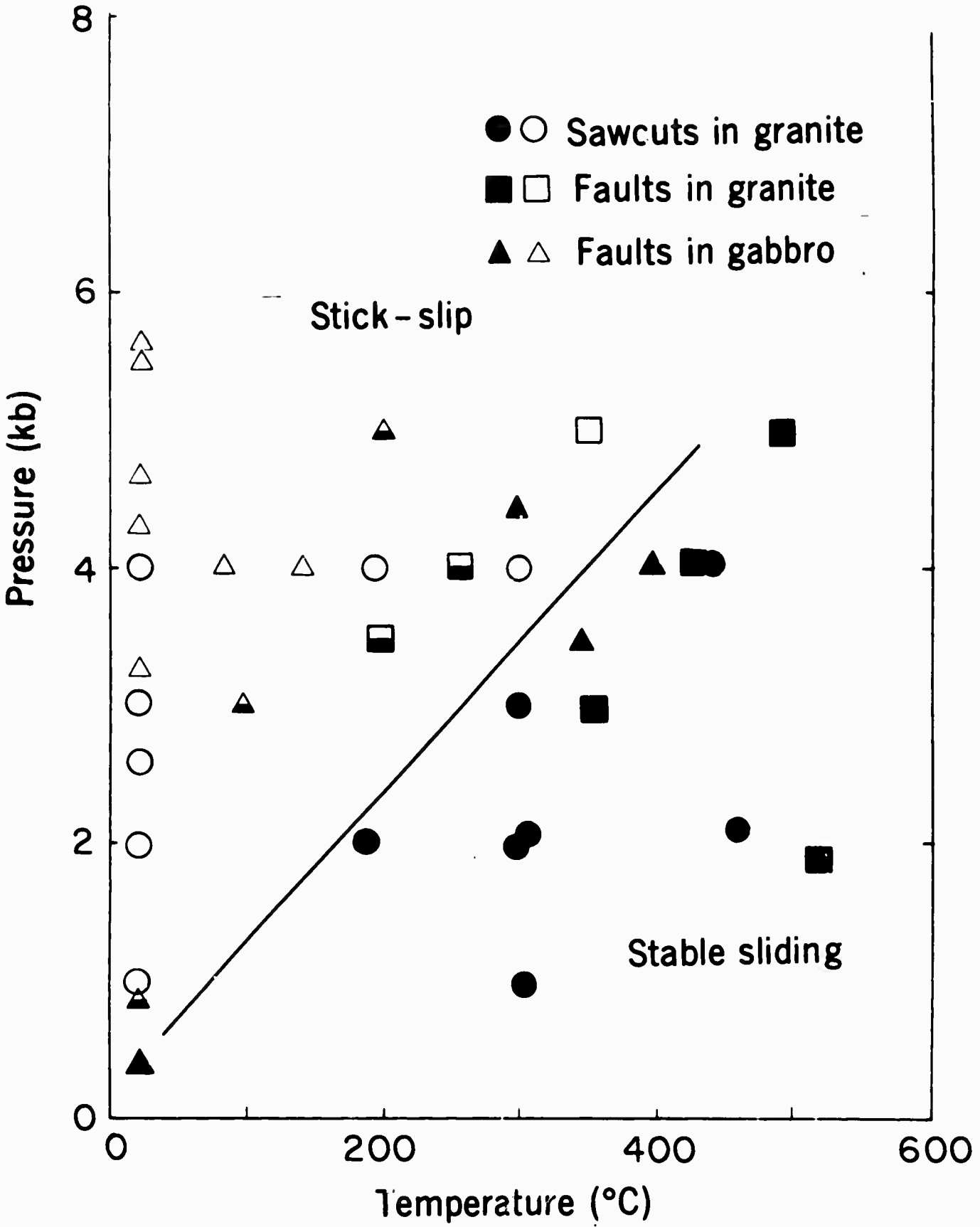
Sawcuts in granite
Faults in granite
Faults in gabbro
Stick-slip
Stable sliding
Pressure (kb)
Temperature (°C)
0
2
4
6
8
0
200
400
600

FIG. 5

At present no physical explanation can be offered for this pronounced effect of temperature on stick-slip. Our understanding of the stick-slip process is still rather incomplete. Byerlee's studies (15) suggest that brittle fracture plays an important role in the frictional behavior of rocks; perhaps an explanation would be apparent if more were known about effect of temperature on brittle fracture of rock-forming minerals. A significant observation from the present work is that frictional strength is lowered by temperature by about the same amount as fracture strength, relative to room temperature values. This suggests that the behavior on a small scale is the same in both cases. The details of this behavior are still obscure.

Before we apply present results to real faults, we need to consider differences which still exist between the laboratory experiment and the field, other than the obvious one of scale. Our experiments will need to be repeated with pore water pressure, for presumably natural rocks are wet. Probably the effective stress law will be followed as it is at room temperature (16). Additional, chemical effects may be present, though, to judge from the water-weakening observed in certain silicate minerals (17). Presumably these will have a further stabilizing influence and shift the field boundary of Figure 3 to the left, to lower temperatures. Slower strain rate than used here need

also be considered; at high temperature some welding or sintering may be expected at very slow strain rates, and this could lead to stick-slip. Further study is needed here, as well. Finally, the effects of displacement will have to be examined more fully. To judge from our observations with faults in gabbro and granite, the nature of the sliding motion changes somewhat with displacement (the middle curve of Figure 4). Some way of obtaining much larger displacements in our laboratory samples is needed.

REFERENCES

1. W.F. Brace and F. Press (1966), Earthquake prediction, Science, 152, 1575.

2. J.P. Eaton, W.H.K. Lee, and L.C. Pakiser (1970), Use of microearthquakes in the study of the mechanics of earthquake generation along the San Andreas fault in central California, Tectonophysics, 9(2/3), 259.

3. B. Isacks, J. Oliver, and L.R. Sykes (1968), Seismology and the new global tectonics, J. Geophys. Res., 73(18), 5855.

4. D. Tocher (1960), Creep rate and related measurements at Vineyard, California, Seismol. Soc. Am. Bull., 50, 396.

5. W.F. Brace and J.D. Byerlee (1966), Stick-slip as a mechanism for earthquakes, Science, 153, 990.

6. J.D. Byerlee and W.F. Brace (1968), Stick-slip, stable sliding and earthquakes, Part 1: Effect of rock type, pressure, strain-rate, and stiffness, J. Geophys. Res., 73(18), 6031.

W.F. Brace (1969), Laboratory studies pertaining to earthquakes, Trans., New York Acad. of Sciences, Ser. II, 31(7), 892.

7. C.R. Allen (1968), The tectonic environments of seismically active and inactive areas along the San Andreas fault system, Proc., Conf. on Geologic Problems of San Andreas Fault System, Stanford Univ. Publ., XI, 70.

8. J.D. Byerlee and W.F. Brace (1970), California earthquakes: Why only shallow focus?, Science, 168(3939), 1573.

9. D.T. Griggs, F.J. Turner, and H.C. Heard (1960), Deformation of rocks at 500° to 800°C, in Rock Deformation (eds. D.T. Griggs and J. Handin), GSA Memoir 79, Ch. 4, 39.

10. W.F. Brace (1968), Current laboratory studies pertaining to earthquake prediction, Tectonophysics, 6(1), 75.

11. J. Handin (1966), Strength and Ductility, in Handbook of Physical Constants (ed. S.P. Clark, Jr.), GSA Memoir 97, Sect. 11, 223.

12. J. Handin and D.W. Stearns (1964), Sliding friction of rock, Trans. Amer. Geophys. Union, 45, 103.

J.D. Byerlee (1967), Frictional characteristics of granite under high confining pressure, J. Geophys. Res., 72(14), 3639.

13. J.D. Byerlee (1967), Frictional characteristics of granite under high confining pressure, J. Geophys. Res., 72(14), 3639.

14. J.D. Byerlee and W.F. Brace (1968), Stick-slip, stable sliding and earthquakes, Part 1: Effect of rock type, pressure, strain-rate, and stiffness, J. Geophys. Res., 73(18), 6031.

15. J.D. Byerlee (1967), Theory of friction based on brittle fracture, J. Appl. Phys., 38(7), 2928.

16. W.F. Brace and R.J. Martin, III (1968), A test of the law of effective stress for crystalline rocks of low porosity, Int. J. Rock Mech.Min.Sci., 5, 415.

17. D.T. Griggs and J.D. Blacic (1965), Quartz: Anomalous weakness of synthetic crystals, Science, 147, 292.